# Omni-drive robot motion on curved paths: The fastest path between two points is not a straight-line

Mark Ashmore and Nick Barnes[1]

Department of Computer Science and Software Engineering
The University Of Melbourne, Vic, 3010, AUSTRALIA
nmb@cs.mu.oz.au[1]

**Abstract.** Omni-drive systems operate by having individual wheels apply torque in one direction in the same way as a regular wheel, but are able to slide freely in another direction (often perpendicular to the torque vector). The key advantage of omni-drive systems is that translational and rotational motion are decoupled for simple motion. However, in considering the fastest possible motion this is not necessarily the case. In this paper, we review all the current popular designs of omni-drive transport systems, and compare them in terms of practical and theoretical considerations. We then present a kinematic analysis that applies to two major omni-drive robot vehicles classes, for any number of wheels. Finally, we show that for three-wheeled omni-drive transport systems and certain ranges of trajectories and starting conditions, a curved path can be traversed faster than a straight-line path, we confirm this result experimentally.

## 1    Introduction

Of mobile robots, wheeled drives are by far the most common means of transportation. Wheeled systems support accurate odometry over smooth flat surfaces. Within the class of wheeled systems, the majority are differential drive, where two parallel wheels execute straight-lines by moving with the same velocity, or curves with differences in velocity. Ackerman steering is common for larger vehicles, particularly road vehicles. However, omni-drive and synchro-drive vehicles have the kinematic advantage of allowing continuous translation and rotation in any direction. Synchro-drive systems have a number of wheels that are aligned in a common direction, and can be turned in any direction. This advantage is apparent for transport systems in confined spaces such as factory floor robots [2]. Also, in competitive high-speed environments, such as the RoboCup competitions, this agility has demonstrated great advantage. For example to move sideways, a differential drive robot can turn 90 degrees, move forward, and then turn back to its original direction. An omni-drive robot can execute a single sideways motion, and further can easily track a moving object while maintaining a required orientation with respect to it, such as following a ball, while maintaining the alignment of a kicking mechanism. Omni-drive robots have the particular advantage of decoupling translational and rotational motion. The kinematics of omni-drive systems are well known [2], and many designs have been published, e.g., six wheels [1], three wheels [4], and four wheels [5]. However, analysis of omni-drive motion on curved paths

has been inadequate to date. Such an analysis is necessary to optimise performance of this type of robot in high-speed competitive domains. That the robot can move in any direction with any rotational velocity is adequate for path planning if speed is not a key consideration, however we want to optimise the performance of the robot for translational paths when rotation is not constrained.

We are interested in optimising robot performance for the Robocup F180 League, a competitive environment where speed is important. Approaches such as the dynamic window [3] can be used to exploit these faster curved paths presented here. The dynamic window was developed on synchro-drive robots.

In this paper, we review omni-directional ground transport systems before examining a particular class of omni-drive vehicles, orthogonal universal wheel-based systems, in more detail. Finally, we look at the motion of omni-drive systems for curved paths. We find that, theoretically, omni-drive systems can travel between points faster for certain curved trajectories than in a straight line. We verify this result experimentally.

## 1.1 Omni-drive transport systems

The basis of the most common omni-drive transport systems is wheels that allow free motion in a direction that is not parallel to the wheel's drive direction. By combining a number of such wheels, each is able to apply a force on the centre of mass of the transport system, and as each wheel has some axis along which it can freely rotate, a velocity can be induced by the other wheels in this direction. The well-known omni-directional transport systems can be separated into two basic classes: orthogonal wheels (pairs of near-spherical wheels), and universal wheels (wheels with rollers).

### 1.1.1 Universal wheels

The universal wheel (see figure 2.1.1) has a set of rollers aligned around its rim that make contact with the ground. Carlisle [2] describes two alternative wheel designs. In the standard design the rollers are aligned so that the wheel can roll freely orthogonally to its driving direction. We will refer to such wheels as orthogonal universal wheels. Platforms with three or more such wheels can produce full omni-directional motion, i.e., arbitrary translation and rotation can be performed, and are decoupled. A second wheel design has the rollers able to free wheel at a non-orthogonal angle to the driving direction of the wheel, typically 45 degrees, e.g., [2,5].

Orthogonal universal wheels are usually placed all at the same distance from the centre of the transport system with their driving direction vector aligned tangentially to the circle connecting them, and with a uniform angle between neighbouring pairs of wheels, see Figure 3.1.2. Both three [2] and four [1] wheeled configurations have been published. The three-wheeled design is mechanically simpler and maintains contact with the ground at all times on rough surfaces, provided there is adequate clearance for the chassis. For the four-wheeled version, suspension is necessary to guarantee contact by all wheels on uneven surfaces, complicating the design. However, in 2002, the Cornel University F180 Robocup team demonstrated that suspension was unnecessary for four wheeled systems if the ground surface is flat.

For transport systems using non-orthogonal universal wheels a minimum of four wheels are required. The standard configuration (e.g., [2,5]) has two rows of two wheels with all driving directions aligned. Forward motion occurs by driving all motors forwards, sideways motion occurs by setting each motor in the opposite direction to its neighbours. Rotation about the centre of mass can be induced by spinning the wheels on one side in the opposite direction of the other side. However, such platforms also require suspension to guarantee ground contact on uneven surfaces, complicating the design. Carlisle also criticises the poor efficiency of the sideways motion [2]. We do not consider this design family further in this paper.

## 1.1.2 Orthogonal wheels

Pin and Killough [6] describe transport systems based on orthogonal wheels. The idea is that a pair of wide, almost spherical, wheels are placed with their axels in orthogonal directions. The wheels are able to rotate freely about their axels. A bracket holds the extremities of the wheel axel, which allows it to be driven to roll on its portion of spherical surface, while free-wheeling in the orthogonal direction. This gives the same effect as the universal wheels. With correctly aligned wheels that are close to spherical, and have synchronised motion, ground contact on one spherical surface or the other is assured at all times while leaving sufficient clearance for the bracket. Thus, an orthogonal pair can drive in one direction and slide in the orthogonal direction. Again, by combining three or more such wheel pairs it is possible to produce omni-directional motion. They present two designs: one where the wheels of a pair are aligned radially from the centre of the robot; and, a more complex design where the wheels of a pair are aligned tangentially. The latter case simplifies the robot kinematics and dynamics because the wheels can be placed such that the point of contact is always a constant distance from the centre of the robot for all wheels.

Watanabe, et. al., [8] present a dynamic model and control scheme for a restricted class of three-wheeled omni-drive robots where the centre of mass is the same distance from the contact points for all wheels. This corresponds to the tangentially aligned pairs variant of Pin and Killough's orthogonal wheel design, where the centre of mass of the robot corresponds to its physical centre (the simplest case of an omni-drive robot for dynamics).

Pin and Killough favour their orthogonal wheels design over the universal wheel-based design. The major reasons given are: the lack of continuous contact with the ground given a single set of rollers; fewer parts; and, a smaller wheel well. These advantages of the orthogonal wheel design have been reduced for builders of mobile platforms of certain sizes by the availability of mass-market universal wheels that are small and reasonably priced. Constructing a platform using pre-manufactured universal wheels (at the sizes for which they are available) is simpler than constructing an orthogonal wheel-base and the size difference when restrictions apply (such as F180 Robocup) is often not significant. Wheels with two rows of rollers, as shown in Figure 2.1.1, ensure smooth contact with the ground, but add a complication for control and odometry in that the point of contact of the wheel moves between the inner and outer row of rollers. However, if the distance between the rollers is small in comparison with the radius of the transport system, the problem remains manageable. Trade-offs like these have currently lead to the greater

popularity of the orthogonal universal wheel design, as can be particularly seen in the small and medium leagues of the Robocup competition [7].

In the remainder of this paper we examine motion models that are common to the orthogonal wheels and the orthogonal universal wheel designs. Previously there has been some study of the motion of a three-wheeled omni-drive robot (e.g. [2,8]), the kinematics for body motion, and dynamics for restricted cases, have been presented. In this paper, we extend this analysis to the kinematics of n-wheeled robots. We also analyse the motion of robots on curved paths, and examine the implications for maximal speed, and experimentally verify the derived results.

## 2    Analysis of omni-drive systems

In this section, we analyse the motion of omni-drive systems. We first describe the motion of a simple two wheeled omni-wheel system. We use this to introduce the velocity augmentation factor, the motion equations, and derive the general case for an n-wheeled system. In this analysis we examine the case of orthogonal universal wheels, however, the analysis is the same for the orthogonal wheels design. This analysis does not apply to non-orthogonal universal wheel-based systems.

## 2.1    A simple omni-wheeled system

A single wheel can only propel itself in the direction of applied force. The simplest possible omni-wheel system that is capable of moving in something other than a straight-line has two wheels attached together so that their directions of driving force are not parallel, as shown in Figure 2.1.1. Due to the angling of the omni-wheels, by varying the speed at which each wheel rotates, we are able to drive the system in any direction we choose. It must be noted at this point that the system described in Figure 2.1.1 is *not* an omni-drive as it is not capable of arbitrary simultaneous translation and rotation, which requires a minimum of three wheels.



**Figure 2.1.1:** Simple omni-wheeled system with angled universal wheels.

## 2.2    Induced velocity

While the system described in Figure 2.1.1 may appear simple, the kinematics are non trivial. The nature of the omni-wheel means that a wheel can obtain a velocity (in its direction of sliding) without applying any driving force itself. The force comes from the motion of the other wheel. We refer to this velocity as **induced velocity**. Consider Figure 2.2.1.
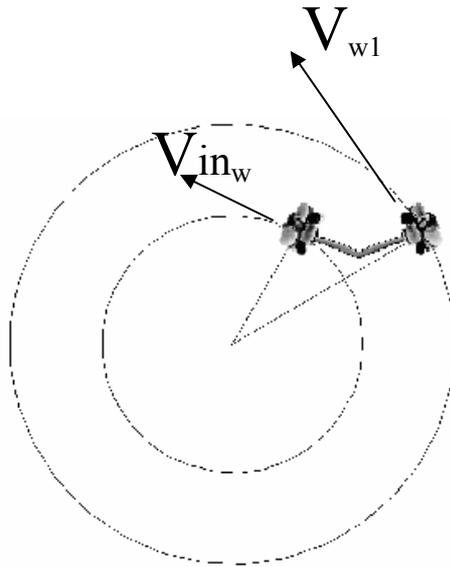
**Figure 2.2.1:** Wheel 1 on the right is driving. Wheel two on the left is locked, $\mathbf{V_{w1}}$ is the velocity of driving wheel one, and $\mathbf{Vin_{w2}}$ is the induced velocity of wheel two.

In Figure 2.2.1, wheel 1 (right) is driving, while wheel 2 (left) is locked, that is cannot rotate about its axle. Assuming no slippage, only rolling in the direction perpendicular to the driving direction of wheel 2 is possible. In this case, the system will rotate about a single point that must lie along a line perpendicular to the velocity of each wheel. The centre of rotation may be found at the intersection of the lines perpendicular to $\mathrm{V}_{w1}$ and $\mathrm{V}in_{w2}$. Wheel 2, which provides *no* driving force, has obtained the velocity $\mathrm{V}in_{w2}$. This is the induced velocity.

## 2.3 Omni-wheeled system motion

We now consider the motion of a simple omni-wheeled system, where rotation is fixed. Consider Figure 2.3.1, showing the vectors acting on one driving wheel.
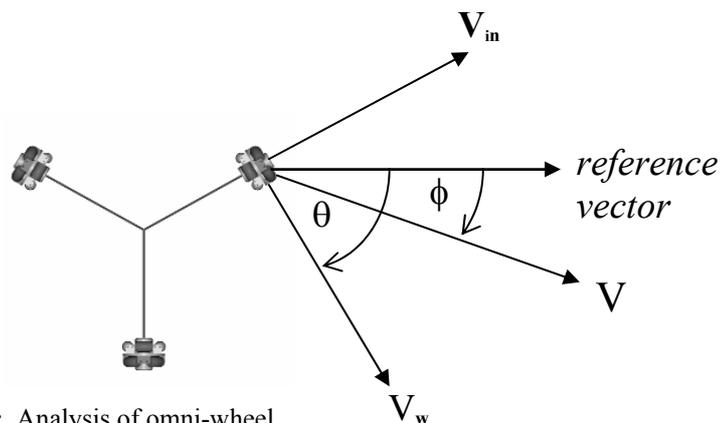


**Figure 2.3.1:** Analysis of omni-wheel

where, $V_w$ is the velocity of the wheel, $\theta$ is the reference wheel angle, $V_{in}$ is the induced velocity on wheel, $\phi$ is the reference body velocity angle, and $V_b$ is the body velocity of robot.

Now $\mathbf{V_{in}}$ and $\mathbf{V_w}$ are always orthogonal:

$$\mathbf{V_b}^2 = \mathbf{V_w}^2 + \mathbf{V_{in}}^2 \tag{1}$$

Also:

$$\mathbf{V_{in}}^2 = \mathbf{V_b}^2 + \mathbf{V_w}^2 - 2\,\mathbf{V_w}\,\mathbf{V_b}\cos(\theta - \phi)$$

$$= \mathbf{V_b}^2 + \mathbf{V_w}^2 - 2\,\mathbf{V_w}\,\mathbf{V_b}\,(\cos\theta\,\cos\phi + \sin\theta\,\sin\phi) \tag{2}$$

Substituting (2) into (1), we may obtain:

$$\mathbf{V_w} = \mathbf{V_b}(\cos\theta\,\cos\phi + \sin\theta\,\sin\phi) \tag{3}$$

For a given rotational velocity of the centre of mass, $\dot{\Psi}$, each wheel must apply velocity:

$$V_w = R\dot{\Psi}, \tag{4}$$

where R is the distance of the wheel from the centre of mass. Thus, for each wheel:

$$V_w = V_b(\cos\theta\cos\phi + \sin\theta\sin\phi) + R\dot{\Psi} \tag{5}$$

This is a general equation that is independent of the number of wheels. Consider a three wheeled omni-directional vehicle with wheels arranged at angles of 0°, 120° and 240°, equation (5) yields:

Wheel 1 ($\theta = 0°$): $\qquad V_{w1} = V_b\cos\phi + R\dot{\Psi}$ $\tag{6}$

Wheel 2 ($\theta = 120°$): $\qquad V_{w2} = V_b(\dfrac{-1}{2}\cos\phi + \dfrac{\sqrt{3}}{2}\sin\phi) + R\dot{\Psi}$ $\tag{7}$

Wheel 3 ($\theta = 240°$): $\qquad V_{w3} = V_b(\dfrac{-1}{2}\cos\phi - \dfrac{\sqrt{3}}{2}\sin\phi) + R\dot{\Psi}$ $\tag{8}$

Similar equations for this three-wheeled case appear in [6]. The translational component only appears also in [2]. As pointed out by Pin and Killough [6], if we separate $V_b$ into x and y components, where $V_{bx} = V_b\cos\phi$, and $V_{by} = V_b\sin\phi$, this becomes a linear relation. We may invert the matrix for any n-wheeled system. Consider, for example, the three-wheeled system above:

$$\begin{bmatrix} V_{bx} \\ V_{by} \\ \dot{\psi} \end{bmatrix} = \begin{bmatrix} \dfrac{-1}{\sqrt{3}} & \dfrac{-2}{3\sqrt{3}} & \dfrac{1}{\sqrt{3}} \\ \dfrac{-1}{3} & \dfrac{-4}{3} & \dfrac{-1}{3} \\ \dfrac{1}{3R} & \dfrac{1}{3R} & \dfrac{1}{3R} \end{bmatrix} \begin{bmatrix} w_1 \\ w_2 \\ w_3 \end{bmatrix} \qquad (9)$$

Now, consider again the system shown in Figure 2.3.1, with initial conditions: $\theta = 60°$, $V_w = 1$, $\phi = 90°$. Substituting these values into Equation (3) gives: $\mathbf{Vb} = 2/\sqrt{3}$

Thus, the addition of angled omni-wheels can result in a net body velocity that is greater than the maximum radial velocity of the wheel. We refer to this additional velocity as the Velocity Augmentation Factor (VAF).
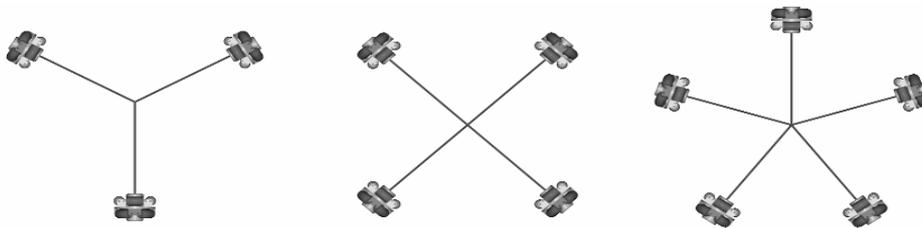


**Figure 2.3.2:** 3, 4 and 5 wheeled omni-drives.

Let us now apply Equation (3), in particular the VAF, to some plausible omni-drive designs, as shown in Figure 2.3.2. Figure 2.3.3 plots the theoretical VAF and average velocity obtained by varying $\phi$ over the range 0° - 360°.
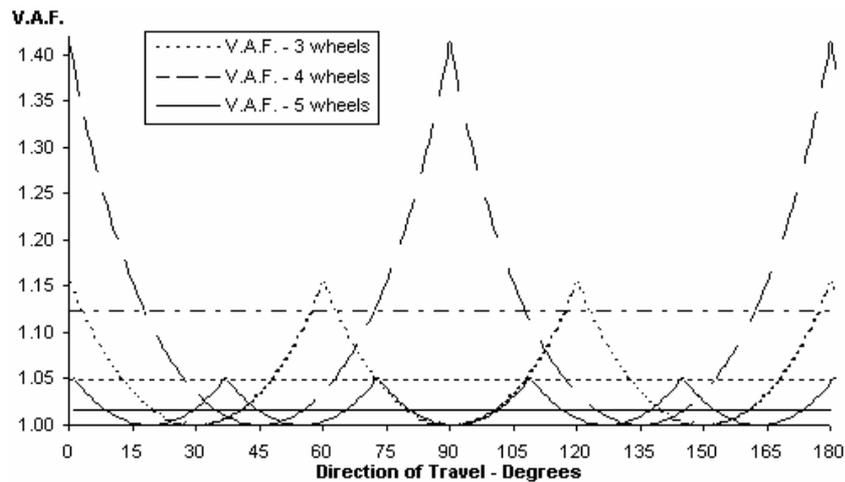


**Figure 2.3.3:** Plots of VAF vs direction for 3, 4 and 5 wheeled omni-drives.

Figure 2.3.3 shows that the four-wheeled design produces the greatest VAF of $\sqrt{2}$ every 90°. Furthermore, as the number of wheels increases above four, while the number of peaks increases, the height of the peaks will always be less than $\sqrt{2}$, as the angle of the relative angle of the wheels affects the VAF.

Consider the configurations shown in Figure 2.3.4 below. The design on the right has a smaller driving angle, that is the interior angle between drive shafts, than the design on the left and so will generate a larger VAF. In the five wheeled omni-drive in Figure 2.3.2 we see that both of these designs are in fact present on the one system. Here, a small driving angle will obtain a large VAF, however, the pair with the large driving angle will not be able to keep up. Since the system as a whole may only go as fast as the pair of wheels with the largest driving angle, any more than four wheels and the VAF is reduced.
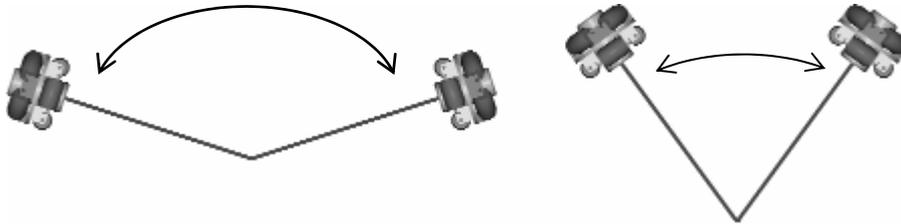


**Figure 2.3.4:** *Example of large (left) and small (right) driving angles.*

## 2.4 Velocity for a three-wheeled omni-drive with rotation

Returning to Figure 2.3.2, we see that for a three-wheeled omni-drive, as used by The University of Melbourne, the maximum VAF is approximately 1.15, however this is only for travel *without* rotation. We may use Equation (9), or its equivalent for higher numbers of wheels to consider the maximum velocity when angular velocity is also allowed. We may take the two components of $V_b$ and combine them to find the total velocity, and set this to a maximum given the maximal velocities for the wheels. We find:

$$V_b^2 = \frac{4}{9}(v_1^2 + v_2^2 + v_3^2 - v_1 v_2 - v_1 v_3 - v_2 v_3) \qquad (10)$$

By maximising Equation (10) we are now able to calculate the maximum possible velocity for the transport system. By inspection, we find that the equation is maximised under the conditions given in Table 2.4.1 below. (Note: All values are in terms of a maximum wheel velocity of 1).

| Velocity | Case 1 | Case 2 | Case 3 |
|----------|--------|--------|--------|
| $V_1$ | $\mp 1$ | $\pm 1$ | $\pm 1$ |
| $V_2$ | $\pm 1$ | $\mp 1$ | $\pm 1$ |
| $V_3$ | $\pm 1$ | $\pm 1$ | $\mp 1$ |
| $Vb$ | 4/3 | 4/3 | 4/3 |

**Table 2.4.1:** *Conditions for maximum body velocity.*

This value 4/3 is greater than, in fact the square of, the maximum VAF ($2/\sqrt{3}$) found previously. We can also see from Equation (9) that there will be a net rotational velocity of the system, i.e., the system will follow a circular path.

We now examine a case where it will be faster to travel a curved path at higher velocity than to travel in a straight line. Figure 2.4.1 shows a curved path D of radius R, and the corresponding direct path d. By calculating d and D and dividing by the maximum speed of traversal, we calculate the time taken to traverse both paths, as follows:
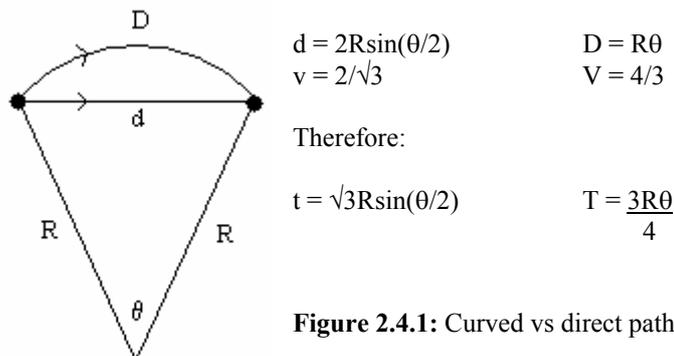


$$d = 2R\sin(\theta/2) \qquad\qquad D = R\theta$$
$$v = 2/\sqrt{3} \qquad\qquad V = 4/3$$

Therefore:

$$t = \sqrt{3}R\sin(\theta/2) \qquad\qquad T = \frac{3R\theta}{4}$$

**Figure 2.4.1:** Curved vs direct paths

Using this information we plot *t* vs *T* to establish when the time taken to travel a curved path is less than the time taken to travel a direct path. This is shown in figure 2.4.2 below. As we can see, for distances under approximately 7.3*r*, where *r* is the radius of the robot, a destination may be reached earlier by travelling a curved path rather than a direct path.
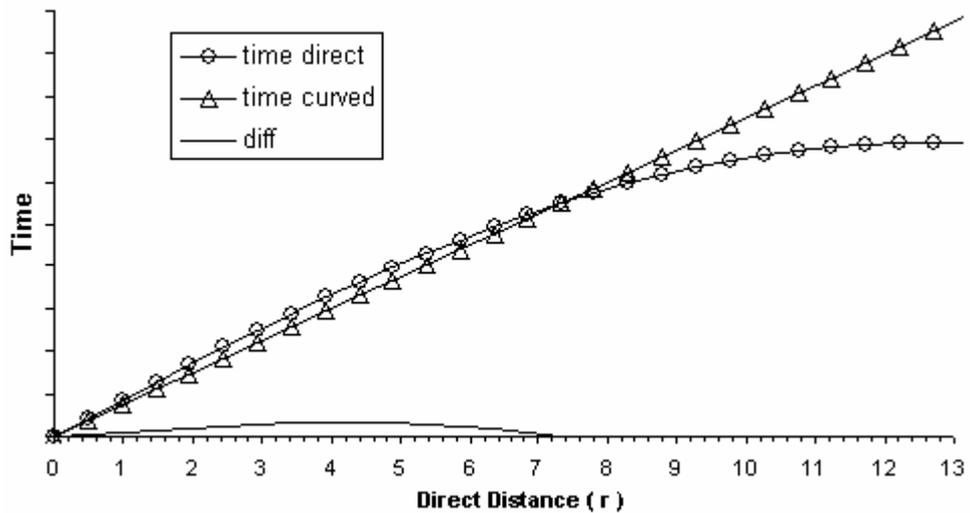
**Figure 2.4.2:** Comparison of direct vs curved path travel times.

This result is for the case of pursuing maximal velocity on both the curved and the straight-line paths. Clearly different rates of curvature with lower translational velocities can also be pursued, however, we do not analyse the other cases here. Also, we have not considered system dynamics. To confirm this result, we now present several experiments.

# 3  Experiments

## 3.1  Experimental Procedure

The experiment was conducted using the robots pictured in figures 3.1.1 and 3.1.2. Each of the three wheels were set to a velocity and allowed to run for a significant period of time. A calibrated overhead camera filmed the robot at a rate of 12.5 frames per second facilitating accurate measurements of the path and velocities. 12 experiments were conducted to test four states of the robot, with each state being tested using three alternate configurations of wheel velocities, as given in table 3.1.1.

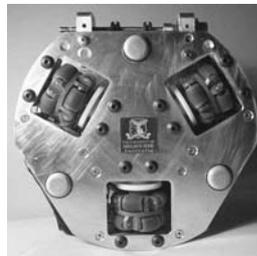

Figure 3.1.1: Side view of robots.



Figure 3.1.2: Base of robot

| State | Wheel Velocities (cm/s) | | |
|-------|------|-------|-------|
| 1 | 12.6 | 0 | 0 |
| 2 | 12.6 | -6.3 | -6.3 |
| 3 | 12.6 | -12.6 | 0 |
| 4 | 12.6 | 12.6 | -12.6 |

**Table 3.1.1:** Experimental wheel velocities.

In state 1, Equation (9) predicts a circular path of radius 2$r$, again where $r$ is the robot radius (in this case 7.5cm), at a VAF of 2/3. States 2 and 3, will result in a straight line path with VAF of 1.00 and 1.15 respectively, while state 4 will induce a circular path of radius 4$r$ at a VAF of 1.33. Table 3.2.1 shows the results. We can see that the robot was able to travel faster along a curved path than in a straight line.

| State | Theoretical VAF | Observed VAF | Error | Theoretical Path Radius (r) | Observed Path Radius (r) | Error |
|-------|------|------|------|------|------|------|
| 1 | 0.67 | 0.69 | 3.0% | 2.00 | 1.73 | 14% |
| 2 | 1.00 | 0.99 | 1.0% | $\infty$ | $\infty$ | N/A |
| 3 | 1.15 | 1.09 | 5.2% | $\infty$ | $\infty$ | N/A |
| 4 | 1.33 | 1.32 | 0.75% | 4.00 | 3.71 | 7.3% |

**Table 3.1.2:** Experiment results.

## 3.2 Experimental Errors

Errors here may be primarily attributed to the control system used to maintain the desired wheel velocity. Each wheel was under position-based control, thus, if the exact wheel velocity is not maintained, the robot will not travel required path or velocity precisely and therefore cause errors. A further irregularity occurs due to dropped frames. This results in large extremes in velocity to be calculated. Such frames generally appear as outliers, and were removed from the results.

It is difficult to precisely quantify these sources of error. However, given that the actual variation from theory across multiple trials was 2.5% on average while the VAF is 33% we view the results as being adequate to support the theory.

## 4 Conclusion

We reviewed omni-drive robot systems and showed the reasons for the popularity of systems based on orthogonal universal wheels. We presented a derivation of a velocity equation for an $n$-wheeled omni-drive robot, valid for these systems as well as systems using the orthogonal wheels design. We introduced the concept of a velocity augmentation factor, and found that the VAF is maximal with a four-

wheeled omni-drive system. We also found that the fastest path between to points, less than 7.3$r$ of the robot, is a curved path for a three-wheeled omni-drive system, given particular starting conditions. These results were verified experimentally.

The curved path result becomes useful when considered in the context of competitive environments such as RoboCup, where optimising paths is of great advantage, especially for points close to the robot. In the Dynamic Window approach [3], the robot searches through a set of possible trajectories to choose the best for the particular situation, given goal direction, current system state (position, orientation and velocities), and neighbouring obstacles. In such an approach we can easily consider that some curved trajectories have different associated velocities. The analysis presented in this paper shows that for certain trajectories and initial conditions curved paths should be considered as faster paths in such an approach.

1. H Asama, M Sato, L Bogoni, H Kaetsu, A. Matsumoto and I. Endo: Development of an Omni-Directional Mobile Robot with 3 DOF Decoupling Drive Mechanism. In IEEE Int. Conf. on Robotics and Automation (1995)
2. B Carlisle: An Omni-Direction Mobile Robot. In B. Rooks, (ed.): Developments in Robotics. IFS Publications/North-Holland Publishing Company. (1983) 79-87
3. D Fox, W Burgard and S Thrun: The Dynamic Window Approach to Collision Avoidance. In IEEE Int. Conf. on Robotics and Automation (1997)
4. K Moore and N Flann: Hierarchical Task Decomposition Approach to Path Planning and Contol for an Omni-Directional Autonomous Mobile Robot. In *IEEE* Int. Symp. on Intelligent Control/Intelligent System & Semiotics, (1999)
5. C Voo: Low Level Driving Routines for the OMNI-Directional Robot, Centre for Intelligent Information Processing Systems, Department of Electrical & Electronic Engineering, The University of Western Australia, Honours Thesis, January (2000)
6. F G Pin and S M Killough: A New Family of Omnidirectional and Holonomic Wheeled Platforms for Mobile Robots, IEEE Transactions on Robotics and Automation **10**(4), Aug (1994) 480-489
7. G A Kaminka, P U Lima, R Rojas (Eds.): RoboCup-2002: Robot Soccer World Cup VI: The 2002 RoboCup Symposium Proceedings. Fukuoka, Japan, June, Springer Verlag (2002)
8. K Watanabe, Y Shiraishi, S G Tzafestas, J Tang, and T Fukuda: Feedback Control of an Omnidirectional Autonomous Platform for Mobile Service Robots. Journ. Intelligent and Robotic Systems, **22** (1998) 315-330